Supporting Information

Conrad et al. 10.1073/pnas.0911253107

SI Materials and Methods

Plasmids, Oligonucleotides, and Proteins. Plasmids and oligonucleotides used for kinetic assays are described in Table S4. Hexahistidine-tagged wild-type and mutant core RNAPs were isolated from *E. coli* BL21 λDE3 *recA* (Invitrogen) transformed with either pRL4455 or pRL4455-derivative plasmids (1) following induction by IPTG, and purified using metal ion affinity chromatography on a Ni-NTA agarose column, followed by chromatography on a heparin column (2). Wild-type and mutant holoenzymes (core ββ′α2 and σ^{70}) were prepared by incubating fivefold molar excess of σ70 with core enzyme for 15 min at 30 °C. Linear DNA templates for in vitro elongation rate assays were obtained by PCR amplification from supercoiled plasmid DNA and purified by QIAspin PCR purification reagents (Qiagen). Plasmids were isolated and purified by Promega reagents.

Cloning of *rpoC* Mutants. The *rpoC* alleles were amplified with Pfu DNA polymerase (Stratagene) from genomic DNA isolated from associated glycerol-adapted strains using PCR primers matching *rpoC* regions that flank SalI and BspEI restriction enzyme sites on plasmid pRL662. *rpoC* alleles were ligated into pRL662 using Quick Ligase (New England Biolabs) following digestion with SalI and BspEI. These alleles were further subcloned into pVS7. Alleles were PCR amplified directly from the modified pRL662 plasmid using primers that flank BsmI and XhoI restriction enzyme sites. Following digestion with BsmI and XhoI, both insert and vector were gel purified. The pVS7 vector fragment was then treated with Antarctic Phosphatase (New England Biolabs) before use in the ligation reaction with the mutant BsmI-XhoI *rpoC* fragment.

Estimation of Biomass. Biomass can be estimated by a linear relationship to OD at 600 nm (3). Previously, a value of 0.44 gDW/L (grams dry weight per liter) per unit OD was used for *E. coli*. We measured in triplicate the biomass of 50-mL cultures of MG1655, del27, eBOP43, and eBOP42 by filtration followed by drying overnight at 60 °C. We determined a conversion of 0.54 gDW/L per unit OD using all data (R^2 = 0.77) and used this value to calculate the values in Table S1. However, MG1655 had values reflecting a coefficient closer to the previously determined value of 0.44 gDW/L per unit OD. Assuming the mutants actually have a higher coefficient than wild type, this complication would only strengthen our inference that biomass yield increases in the mutants.

In Vitro Transcriptional Pause Assay. Wild-type and mutant ECs were reconstituted 2 nt upstream from the pause site as described previously (4). RNA/DNA scaffolds were assembled in reconstitution buffer [20 mM Tris-HCl (pH 7.9), 20 mM NaCl, 0.1 mM EDTA] by heating 2 μM nontemplate strand DNA, 1 μM template strand DNA, and 1 μM RNA for 2 min at 75 °C, rapidly cooling to 45 °C, and then cooling to room temperature in 1 °C/min decrements. To form ECs, 100 nM core RNAP was incubated with 50 nM RNA/DNA scaffold in the same buffer plus 5% glycerol, 10 mM $MgCl_2$, 1 mM DTT, 20 μg acetylated BSA/mL for 10 min at 22 °C, and then incubated 15 min at 37 °C.

Reconstituted EC27 was incubated with 0.17 μM [α-^{32}P]-CTP for 2 min at 37 °C to form the EC28 halted 1 nt before the pause site, and then incubated with 10 μM unlabeled CTP and 10 μM UTP for an additional 15 min to form the EC29 paused complex. Transcription was restarted by addition of 5 μM GTP. Samples were removed at different time points and quenched by the addition of an equal volume of 2× STOP buffer [10 M urea, 98 mM Tris borate (pH 8.3), 25 mM Na_2EDTA, 0.05% bromophenol blue]. Samples were heated for 2 min at 94 °C and separated by electrophoresis although 15% denaturing polyacrylamide (19:1) gels [7 M Urea, 45 mM Tris-borate (pH 8.3), 1.25 mM EDTA]. The pause half-life was calculated by nonlinear regression analysis of the rate of escape from the pause site.

In Vitro Elongation Rate Assay. The in vitro elongation rate was determined using the standard conditions as described previously (5). Halted elongation complexes were formed with 25 nM linear T7 A1 promoter DNA template and 40 nM RNAP holoenzyme in transcription buffer [20 mM Tris-HCl, 20 mM NaCl, 3 mM $MgCl_2$, 14 mM 2-mercaptoethanol, 0.1 mM EDTA (pH 7.9)]. ECs were halted at position A29 by incubation with 150 μM ApU, 10 μM ATP, 10 μM GTP, 10 μM [α-^{32}P]-CTP (32.5 Ci/mmol) for 15 min at 37 °C. Transcription was restarted by addition of 150 μM NTPs and rifampicin to 100 μg/mL Samples were removed at different time points and quenched with an equal volume of 2× STOP buffer and analyzed as described. The elongation rate was calculated from the time required for 50% of halted elongation complexes to make full-length RNA product.

Lifetimes of Open Complexes. Open complexes were formed by incubation of 10 nM RNAP holoenzyme with 2 nM promoter template (supercoiled plasmid containing a *rrnB P1* transcription template that produces a 157-nt transcript) for 10 min at 30 °C in transcription buffer [40 mM Tris-HCl (pH 7.9), 10 mM $MgCl_2$, 1 mM DTT, 0.1 μg acetylated BSA/μL, 50 mM NaCl]. ppGpp (100 μM), DksA (100 nM), or both was present as indicated in the figure legends. At time 0, 200 nM of a 60 nt double-stranded DNA fragment containing the *full con* promoter was added as a competitor (6). At different times thereafter, 10-μL aliquots of the reaction were added to tubes containing 1.25 μL NTPs [final concentration 500 μM ATP, 200 μM CTP, 200 μM GTP, 10 μM [α-^{32}P]-UTP (10 Ci/mmol)] and incubated an additional 10 min. Samples were quenched with an equal volume of 2× STOP buffer and analyzed as described. The open complex half-life was calculated by nonlinear regression analysis of the relative rate of decrease in *rrnB* P1 transcript over time.

RNA Polymerase ChIP-chip. Triplicate MG1655 wild-type and del27 mutant batch cultures in GMM were harvested during midlog growth phase (OD $A_{600} \approx 0.3$) and cross-linked by incubation in 1% formaldehyde (37% solution; Fisher Scientific) at room temperature for 25 min. Following quenching the unused formaldehyde with 125 mM glycine at room temperature for an additional 5-min incubation, the cross-linked cells were harvested and washed three times with 50 mL of ice-cold TBS. The washed cells were resuspended in 0.5 mL lysis buffer composed of 50 mM Tris-HCl (pH 7.5), 100 mM NaCl, 1 mM EDTA, protease inhibitor mixture (Sigma), and 1 kU Ready-Lyse™ lysozyme (Epicentre). The cells were incubated at 37 °C for 30 min and then treated with 0.5 mL of 2× IP buffer composed of 100 mM Tris-HCl (pH 7.5), 200 mM NaCl, 1 mM EDTA, and 2% (vol/vol) Triton X-100. The lysate was then sonicated four times for 20 s each in an ice bath to fragment the chromatin complexes using a Misonix Sonicator 3000 (output level = 2.5). Cell debris was removed by centrifugation at 37,000 × *g* at 4 °C for 10 min, and the resulting supernatant was used as cell extract for the immunoprecipitation.

To immunoprecipitate the RNAP-DNA complexes, 6 μL of anti-RNAP β-subunit mouse antibody (Neoclone) was added to

the cell extract. For the control (mock-IP), 2 μg of normal mouse IgG (Upstate) was added into the cell extract. Reactions were then incubated at 4 °C overnight, and 50 μL of washed Dynabeads Pan Mouse IgG or protein A magnetic beads (Invitrogen) were added to the mixture. After a 5-h incubation at 4 °C, the beads were washed, in order, twice with the IP buffer [50 mM Tris-HCl (pH 7.5), 140 mM NaCl, 1 mM EDTA, and 1% (vol/vol) Triton X-100], once with wash buffer I [50 mM Tris-HCl (pH 7.5), 500 mM NaCl, 1% (vol/vol) Triton X-100, and 1 mM EDTA], once with wash buffer II [10 mM Tris-HCl buffer (pH 8.0), 250 mM LiCl, 1% (vol/vol) Triton X-100, and 1 mM EDTA], and once with TE buffer [10 mM Tris-HCl (pH 8.0), 1 mM EDTA]. After removing the TE buffer, the immunoprecipitated DNA protein complexes were eluted from the beads in 200 μL of elution buffer [50 mM Tris-HCl (pH 8.0), 10 mM EDTA, and 1% SDS] and incubated at 65 °C overnight for reverse cross-linking.

After reversal of the cross-links, RNA was removed by incubation with 200 μL TE buffer with 1 μL of RNaseA (Qiagen) for 2 h at 37 °C. Proteins in the DNA sample were then removed by incubation with 4 μL of proteinase K solution (Invitrogen) for 2 h at 55 °C. The sample was then purified with a PCR purification kit (Qiagen). Before shipment to NimbleGen, where sample labeling, microarray hybridization, and visualization steps were carried out, gene-specific quantitative PCR was carried out for promoter regions of *gapA*, *tpi*, *fbp*, *pgi*, and *dmsA* using the isolated DNA samples as template to confirm immunoprecipitation quality.

The NimbleGen array contained 50-mers with 25-bp overlap, covering the MG1655 genome forward and reverse strands. Separately labeled anti-RNAP and mock samples were hybridized to the array. Nimblegen performed normalization of raw data (paired files) by subtracting the biweight mean for the log-ratio values. Data quality was checked by calculating the Pearson correlation efficient of replicates (>0.95) and ensuring similar data distributions.

Binding to rRNA transcription units was determined by calculating the average signal over the genomic coordinates of the ribosomal operons as listed in EcoCyc (http://ecocyc.org/) (7): rrsA-ileT-alaT-rrlA-rrfA (rrsAp1) 4033262–4038659; rrsB-gltT-rrlB-rrfB (rrsBp1) 4164390–4169779; rrsC-gltU-rrlC-rrfC (rrsCp1) 3939539–3944842; rrsD-ileU-alaU-rrlD-rrfD-thrV-rrfF (rrsDp1) 3421564–3427069; rrsE-gltV-rrlE-rrfE (rrsEp) 4205886–4211063; rrsE-gltV-rrlE-rrfE (rrsEp) 2724210–2729470; rrsH-ileV-alaV-rrlH-rrfH (rrsHp1) 223485–228875. Because amounts of both forward-strand and reverse-strand immunoprecipitated DNA should be approximately equal, both strands were used for quantifying RNAP binding. For each replicate, the sum of signal across the ribosomal transcription units was normalized by the sum of signal across the genome. The normalized value was averaged across three biological replicates. Statistical significance of the difference in ribosomal binding signal between the MG1655 samples and the del27 samples was determined using a two-sample *t* test.

Gene Expression: GO Class, COG, and Regulon Enrichment. For each gene, the associated Gene Ontology (GO) classes, COGs, and regulons were determined. GO classes were obtained from EcoCyc v 12.0 (7); COGs were obtained from the COG database (8); and regulon structure was determined from RegulonDB 6.0 (9). Enrichment within clusters and differentially expressed genes was determined using the hypergeometric test (false discovery rate: 0.05).

Motility Assays. Strains were grown to stationary phase in glycerol minimal media and then spotted onto 0.2% agar, 2 g/L glycerol + M9 salts plates and incubated at 30 °C. Plates were photographed after 24, 48, and 72 h. A strain was considered motile if its halo expanded between 24 and 48 h in at least three of five replicates. A similar method to determine motility was described in ref. 10.

1. Toulokhonov I, Zhang J, Palangat M, Landick R (2007) A central role of the RNA polymerase trigger loop in active-site rearrangement during transcriptional pausing. *Mol Cell* 27:406–419.
2. Wang D, et al. (1995) Discontinuous movements of DNA and RNA in RNA polymerase accompany formation of a paused transcription complex. *Cell* 81:341–350.
3. Fong SS, Nanchen A, Palsson BO, Sauer U (2006) Latent pathway activation and increased pathway capacity enable *Escherichia coli* adaptation to loss of key metabolic enzymes. *J Biol Chem* 281:8024–8033.
4. Kyzer S, Ha KS, Landick R, Palangat M (2007) Direct versus limited-step reconstitution reveals key features of an RNA hairpin-stabilized paused transcription complex. *J Biol Chem* 282:19020–19028.
5. Ederth J, Artsimovitch I, Isaksson LA, Landick R (2002) The downstream DNA jaw of bacterial RNA polymerase facilitates both transcriptional initiation and pausing. *J Biol Chem* 277:37456–37463.
6. Gaal T, et al. (2001) Promoter recognition and discrimination by EsigmaS RNA polymerase. *Mol Microbiol* 42:939–954.
7. Keseler IM, et al. (2009) EcoCyc: a comprehensive view of *Escherichia coli* biology. *Nucleic Acids Res* 37(Database issue):D464–D470.
8. Tatusov RL, et al. (2003) The COG database: An updated version includes eukaryotes. *BMC Bioinformatics* 4:41.
9. Gama-Castro S, et al. (2008) RegulonDB (version 6.0): Gene regulation model of *Escherichia coli* K-12 beyond transcription, active (experimental) annotated promoters and Textpresso navigation. *Nucleic Acids Res* 36(Database issue): D120–D124.
10. Sperandio V, Torres AG, Kaper JB (2002) Quorum sensing *Escherichia coli* regulators B and C (QseBC): A novel two-component regulatory system involved in the regulation of flagella and motility by quorum sensing in *E. coli*. *Mol Microbiol* 43:809–821.
11. Chlenov M, et al. (2005) Structure and function of lineage-specific sequence insertions in the bacterial RNA polymerase beta' subunit. *J Mol Biol* 353:138–154.
12. Traxler MF, et al. (2008) The global, ppGpp-mediated stringent response to amino acid starvation in *Escherichia coli*. *Mol Microbiol* 68:1128–1148.

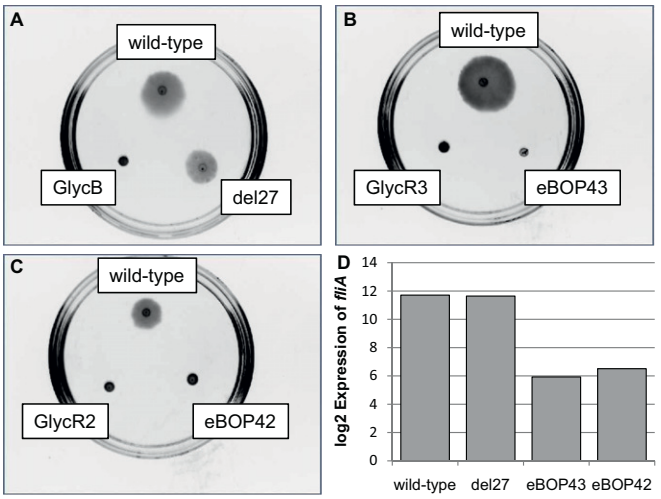

Fig. S1. Motility changes in RNAP mutants. Motility was assayed by a standard method using soft agar (0.2%) plates containing glycerol and M9 salts. Five replicates were used for each strain. A strain was called motile if a halo developed around the spot of inoculation after 48–72 h in at least three replicates. Wild-type MG1655 consistently showed motility after 48 h. (*A*) del27 was the only motile RNAP mutant among those studied; however, GlycB, the glycerol-adapted strain in which del27 was originally identified, is not motile, presumably due to presence of other mutations. (*B* and *C*) The other two mutants, eBOP43 and eBOP42, as well as their respective glycerol-adapted strains, GlycR3 and GlycR2, are nonmotile. Motility in the RNAP mutants correlated with the expression of *fliA* as measured by microarrays. The *fliA* gene codes the sigma factor for motility and chemotaxis genes, σ^{28}.

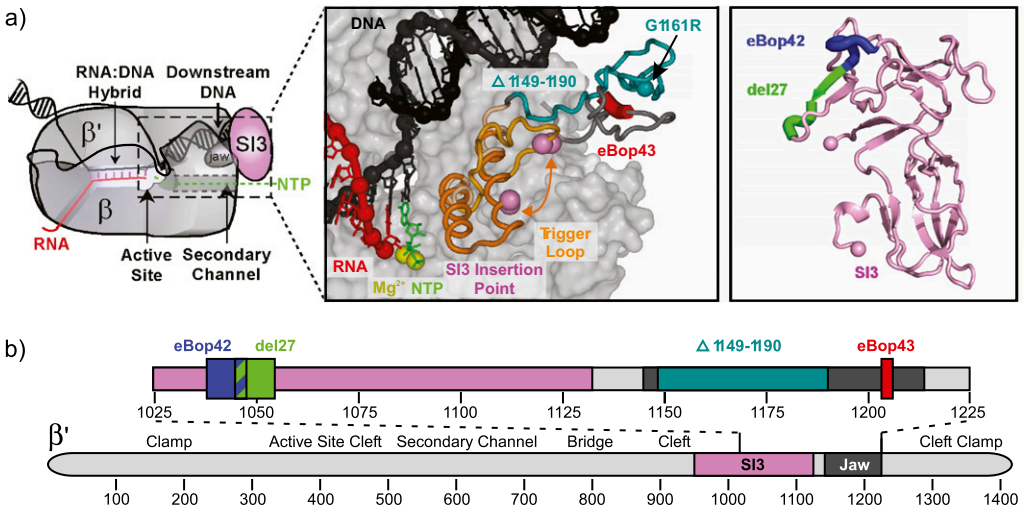

Fig. S2. The structure of the transcription elongation complex and the location of the small deletions in the β′ subunit of RNAP. (*A, Left*) Diagram of the transcription elongation complex. (*Center*) Structure of the RNAP active site (1). Transcription occurs left to right. DNA, black; RNA, red; Mg^{2+} ions, yellow; incoming nucleotide, green; β′ subunit, light gray semitransparent surface; trigger loop, orange; SI3 insertion point, pink spheres; jaw domain, dark gray; previously identified jaw substitution and deletion (5), teal; eBop43 deletion, red. (*Right*) Structure of SI3 (11). SI3, pink; ebop42 deletion, blue; del27 deletion, green. (*B*) The context of the small deletions of interest in the β′ subunit polypeptide. The positions of the deletions in the β′ polypeptide are indicated by colored rectangles.

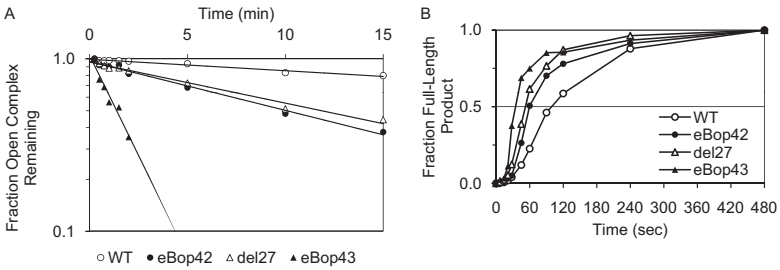

Fig. S3. The small deletions in *rpoC* alter RNAP kinetics in vitro. (*A*) Comparison of open complex longevity at the *rrnB* P1 promoter. RPo longevity was assayed on supercoiled pRLG6555 using a single round transcription assay. Plot of the relative fraction of RPo remaining as a function of time in the absence of ppGpp/DksA. Each point represents the average of three or more experiments. (*B*) Comparison of in vitro transcription elongation rate. Elongation was assayed by synchronized transcription on a linear T7 A1 promoter template containing a fragment of the *E. coli rpoB* gene. The graph shows a plot of the fraction of full-length RNA products as a function of time. Each point represents the average of three experiments.

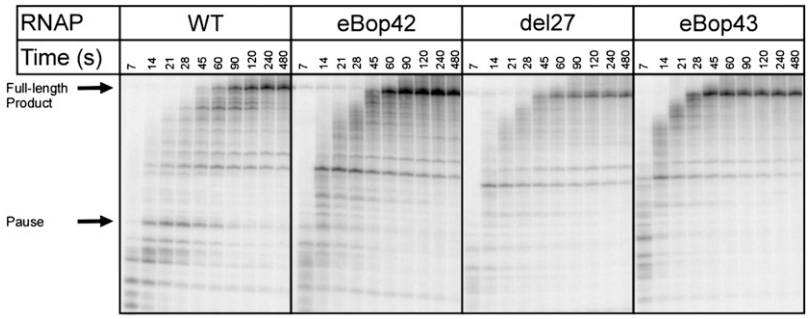

Fig. S4. The small deletions in *rpoC* increase in vitro elongation rate and decrease pausing. Electrophoretic separation of RNAs formed during in vitro elongation on the linear *rpoB* template as a function of time. The prominent pause bands are suppressed by the mutant RNAPs, as indicated by the observed disappearance of the band indicated by the arrow in the figure.

Table S1. Physiological measurements

Table S1

Columns 2–4 show the growth rate of several strains in M9 minimal media with various carbon sources (glycerol, glucose, and L-lactate) determined in triplicate and reported in units of 1/h. Column 5 shows the slower growth of the RNAP mutants in a rich medium. Data in columns 6–8 were generated in part by measurements of glycerol and acetate in the culture filtrate using HPLC. Biomass is estimated by measurement of OD at 600 nm. Column 8 summarizes the motility measurements presented in Fig. S1. gDW: grams dry weight; n.d., not determined.

Table S2. Data used to generate the clustergram in Fig. 2*C*

Table S2

The l2r (log2 ratio) values in columns 4–6 were calculated by subtracting the average (log2 scale) MG1655 signal for each gene from the average mutant signal.

Table S3. Comparison of significantly differentially expressed genes in the RNAP mutants to significantly differentially expressed genes in a stringent response

Table S3

Column 3 is derived from column 4 (log2 expression ratio of isoleucine starved WT **vs.** unstarved WT) of **t**able S1 from Traxler et al. (**12**). The log2r (log2 ratio) values in columns 4–6 were calculated by subtracting the average (log2 scale) MG1655 signal for each gene from the average mutant signal. The data are sorted vertically into four categories (with genes within each category sorted alphabetically): the top category contains genes that are on average down-regulated in both a stringent response (stringent response **vs.** no stringent response) and the mutants (mutant **vs.** MG1655); the next category down contains genes that are on average up-regulated in both a stringent response and the mutants; the third category down contains genes that are on average up-regulated in a stringent response and down-regulated in the mutants; the bottom category contains genes that are on average down-regulated in a stringent response and up-regulated in the mutants. Only genes that are significantly differentially expressed in both a stringent response and the mutants are included in the table.

Table S4. Plasmids and oligonucleotides

Table S4